Front. Environ. Sci. Eng. 2018, 12(1): 4
DOI 10.1007/s11783-017-0977-8

RESEARCH ARTICLE

Fabrication and photocatalytic ability of an Au/TiO_2/reduced graphene oxide nanocomposite

Fenghe Lv[1,2], Hua Wang (✉)[1,2,3], Zhangliang Li[3], Qi Zhang[1,4], Xuan Liu[1,4], Yan Su (✉)[4]

1 School of Fisheries and Life Science, Dalian Ocean University, Dalian 116023, China
2 Key Laboratory of Mariculture & Stock Enhancement in North China's Sea, Ministry of Agriculture, Dalian 116023, China
3 Fujian Provincial Key Laboratory of Ecology-Toxicological Effects & Control for Emerging Contaminants, Putian 351100, China
4 Faculty of Chemical, Environmental and Biological Science and Technology, Dalian University of Technology, Dalian 116024, China

HIGHLIGHTS

- Deposition Au nanoparticles on both TiO_2 and RGO to fabricate Au/TiO_2/RGO.
- Au/TiO_2/RGO displayed a high H_2O_2 and •OH production in photocatalytic process.
- RGO is a good collector to transfer electrons from TiO_2 to Au.

GRAPHIC ABSTRACT

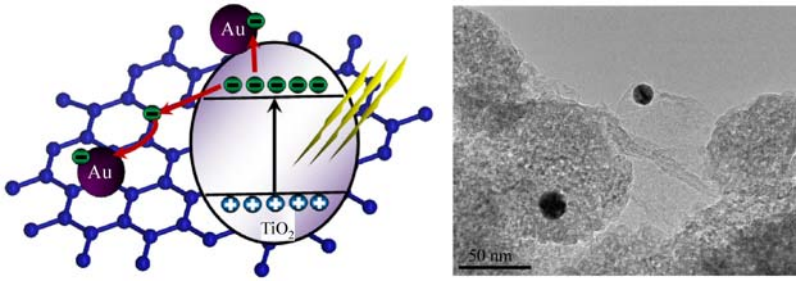

ARTICLE INFO

Article history:
Received 22 February 2017
Revised 23 April 2017
Accepted 18 June 2017
Available online 28 July 2017

Keywords:
Reduced graphene oxide
Au
TiO_2
Nanocomposite
Photocatalysis

ABSTRACT

A new type of Au/TiO_2/reduced graphene oxide (RGO) nanocomposite was fabricated by the hydrothermal synthesis of TiO_2 on graphene oxide followed by the photodeposition of Au nanoparticles. Transmission electron microscopy images showed that Au nanoparticles were loaded onto the surface of both TiO_2 and RGO. Au/TiO_2/RGO had a better photocatalytic activity than Au/TiO_2 for the degradation of phenol. Electrochemical measurements indicated that Au/TiO_2/RGO had an improved charge transfer capability. Meanwhile, chemiluminescent analysis and electron spin resonance spectroscopy revealed that Au/TiO_2/RGO displayed high production of hydrogen peroxide and hydroxyl radicals in the photocatalytic process. This high photocatalytic performance was achieved via the addition of RGO in Au/TiO_2/RGO, where RGO served not only as a catalyst support to provide more sites for the deposition of Au nanoparticles but also as a collector to accept electrons from TiO_2 to effectively reduce photogenerated charge recombination.

1 Introduction

TiO_2 is considered one of the most attractive photocatalysts due to its extraordinary semiconducting properties, such as high photocatalytic ability, remarkable chemical stability, environmental friendliness and cost effectiveness [1,2]. Because of these unique properties, TiO_2 has been applied in photocatalysis [3], sensors [4] and solar cells [5]. However, the photocatalytic efficiency of TiO_2 is still low because of the rapid recombination of photogenerated electrons and holes [6,7]. To reduce the probability of electron-hole recombination, an attempt of loading Au nanoparticles on the surface of TiO_2 as a cocatalyst was proposed to form a nanocomposite of Au/TiO_2. The recombination of photogenerated electrons and holes might be inhibited by the built-in electric field at the interface of the metal and semiconductor, and the excited electrons generated from TiO_2 might migrate into the Au nanoparticles [8–10].

Graphene, a single atomic layer carbon nanostructure, is regarded as a promising photocatalyst support because of

✉ Corresponding authors
E-mail: wanghua@dlou.edu.cn (Wang H); susu@dlut.edu.cn (Su Y)

its superior electrical conductivity, good optical transparency, remarkable chemical stability and high specific surface area [11–13]. In particular, it has been reported that a high photocatalytic activity could be achieved using graphene as an ideal photogenerated electron transporter to efficiently increase the separation of photogenerated electrons and holes [14–16]. Motivated by the distinguished properties of graphene, we expect that single atomic layer graphene could also serve as a promising support for TiO_2 and Au nanoparticles, attaching to form a nanocomposite of Au/TiO_2/graphene. In this nanocomposite, Au nanoparticles could be loaded onto the surface of both TiO_2 and graphene, which will give the photogenerated electrons two transfer routes. As shown in Fig. 1, if Au nanoparticles are combined with TiO_2, photogenerated electrons could directly migrate from TiO_2 into Au. Meanwhile, if Au nanoparticles are loaded onto the surface of graphene, photogenerated electrons could first migrate from TiO_2 to graphene, then the photogenerated electrons could continually migrate from graphene to Au since graphene would benefit from the transported photogenerated charge carriers [17]. This indicates that the separation of photogenerated electrons and holes could be further increased in Au/TiO_2/graphene nanocomposites on behalf of the participation from graphene. However, until now, less attention has been paid to the application of graphene as a support for the preparation of Au/TiO_2/graphene nanocomposites [18]. Here, we explore an approach to load Au nanoparticles on the surface of TiO_2/graphene to fabricate Au/TiO_2/graphene nanocomposites. The influence of graphene on the properties of Au/TiO_2/graphene was investigated, and the photocatalytic activity of these nanocomposites was evaluated for the photodegradation of phenol.

2 Materials and methods

2.1 Preparation of Au/TiO_2/graphene nanocomposite

The process for the preparation of the Au/TiO_2/graphene nanocomposite included graphene oxide fabrication, TiO_2/reduced graphene oxide (RGO) hydrothermal synthesis and photodeposition of Au on TiO_2/RGO. Briefly, the graphene oxide used for the fabrication of the Au/TiO_2/RGO nanocomposites was produced by chemical oxidation of natural graphite powder in concentrated H_2SO_4 and $KMnO_4$. Then, a varying amount of the prepared graphene oxide and P25 were dispersed in deionized water. The weight ratios of graphene oxide to P25 were 0.5%, 1.0%, and 1.5%. Each solution was transferred into an autoclave and held at 160°Cfor 3 h. After the hydrothermal reaction, the obtained samples were rinsed with deionized water and dried in an oven at 60°C for 12 h. The obtained samples were labeled TiO_2/0.5RGO, TiO_2/1.0RGO, and TiO_2/1.5RGO. Finally, 0.5 g of prepared TiO_2/RGO and 16 mmol $HAuCl_4$ were dispersed in 100 mL of a mixed solution of alcohol and deionized water (volume ratio of 1:1). The solution was irradiated with a Xe lamp under vigorous stirring at 20°C for 1 h. After that, the precipitates from the mixture were collected by centrifugation. The final products of Au/TiO_2/RGO were dried overnight at room temperature. For comparison, a sample of Au/TiO_2 was prepared under the same experimental conditions using P25 as a precursor instead of TiO_2/RGO.

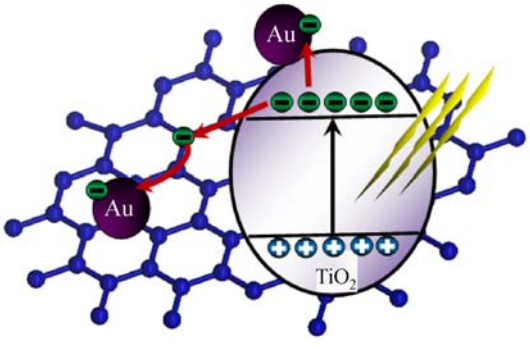

Fig. 1 A schematic mechanism of photogenerated electrons migrating in the Au/TiO_2/graphene nanocomposite

2.2 Characterization

The general morphologies of the prepared samples were observed by transmission electron microscopy (TEM, FEI Tecnai G^2 F30, USA). The crystallinity of the products was determined by X-ray diffraction (XRD) using a diffractometer (Shimadzu LabX XRD-6000, Japan). The Raman spectra were obtained using a Renishaw Micro-Raman System 2000 Spectrometer. The electrochemical impedance spectroscopy (EIS) plots were measured in the dark or under UV irradiation using an electrochemical station (CHI660D, Shanghai Chenhua Limited, China).

2.3 Photocatalytic activity

The photocatalytic activity of Au/TiO_2/RGO was investigated for the photocatalytic degradation of phenol (initial concentration of 10 $mg \cdot L^{-1}$). A high-pressure mercury lamp (300 W) was used as the light source with a principal wavelength of 365 nm. The incident light intensity was 0.75 $mW \cdot cm^{-2}$, which was measured by a radiometer (model UV-A, Photoelectric Instrument Factory Beijing Normal University, China). All the experiments were carried out at room temperature (approximately 25°C) in a cylindrical quartz reactor with a magnetic stirrer set to a constant speed. The volume of the phenol solution was 100 mL with 20 mg prepared photocatalyst. At certain time intervals, 1.5 mL of the solution was collected and filtered to remove the photocatalyst for analysis. The concentration of phenol was detected by high-performance liquid chromatography (HPLC, Waters 2695, USA). In addition,

during the photocatalytic process, a flow injection apparatus (IFIS-D, Xi'an Remex Analysis Instrument Co. Ltd., China) combined with the detector of a chemiluminescence system (MIP-B, Xi'an Remex Analysis Instrument Co. Ltd., China) was used for the determination of hydrogen peroxide (H_2O_2) [19], and hydroxyl radicals (•OH) were recorded on an electron spin resonance spectrometer (ESR, Bruker Elexsys A 200, Germany) using 5,5-dimethyl-1-pyrroline-N-oxide (DMPO) as the spin-trap reagent.

3 Results and discussion

3.1 Characterization of Au/TiO_2/RGO

The morphologies of TiO_2/RGO and Au/TiO_2/RGO were observed by TEM to directly investigate the structure of TiO_2/RGO decorated with Au nanoparticles. Figure 2(a) shows that TiO_2 particles are present on RGO, indicating RGO served as a good support. After the deposition of the Au nanoparticles, it can be seen from Fig. 2(b) that the Au nanoparticles were loaded on the surface of both TiO_2 and RGO, indicating that the aggregation of the Au nanoparticles was inhibited. Meanwhile, Fig. 2(c) shows that the size of the Au nanoparticles in Au/TiO_2/RGO is approximately 20 nm.

Figure 3 shows the XRD patterns of TiO_2/RGO and Au/TiO_2/RGO. For TiO_2/RGO, the typical strong peak of TiO_2 was found at 25.3°, and several weak diffraction peaks matched those of the crystalline anatase phase of TiO_2 (JCPDS card No. 21-1272). Meanwhile, a rutile phase was also observed at 27.2°, indicating that anatase TiO_2 was the majority phase mixed with a minute quantity of the rutile phase [20]. However, no characteristic peak for RGO could be indexed. Compared with that of TiO_2/RGO, the XRD pattern of Au/TiO_2/RGO showed four additional peaks at 2θ values of 38.2°, 44.2°, 64.8°, and 78.0°, corresponding to the (111), (200), (220), and (311) diffraction planes of Au, respectively [18].

Figure 4 shows the Raman spectra of Au/TiO_2, Au/TiO_2/0.5RGO, Au/TiO_2/1.0RGO, and Au/TiO_2/1.5RGO. In these spectra, the typical spectral features for the anatase phase of TiO_2 were found at approximately 145, 395, 515, and 637 cm^{-1} [3]. Compared with Au/TiO_2, two frequencies at approximately 1343 cm^{-1} (D band) and 1586 cm^{-1} (G band) were observed for all Au/TiO_2/RGO samples, confirming the presence of RGO in the Au/TiO_2/RGO nanocomposites [21]. Meanwhile, with an increase in the proportion of RGO in Au/TiO_2/RGO, the intensity of the TiO_2 peaks decreased, and the intensities of the RGO peaks increased. This occurred due to the increasing proportion of RGO in the Au/TiO_2/RGO nanocomposite reducing the influence of TiO_2 on the Raman measurement. These results, in accordance with the XRD measurements, agree well with the TEM observations.

3.2 Photocatalytic activity of Au/TiO_2/RGO

The performance of Au/TiO_2/RGO was evaluated by the photocatalytic degradation of phenol (10 $mg \cdot L^{-1}$) under UV light irradiation. For comparison, the photocatalytic

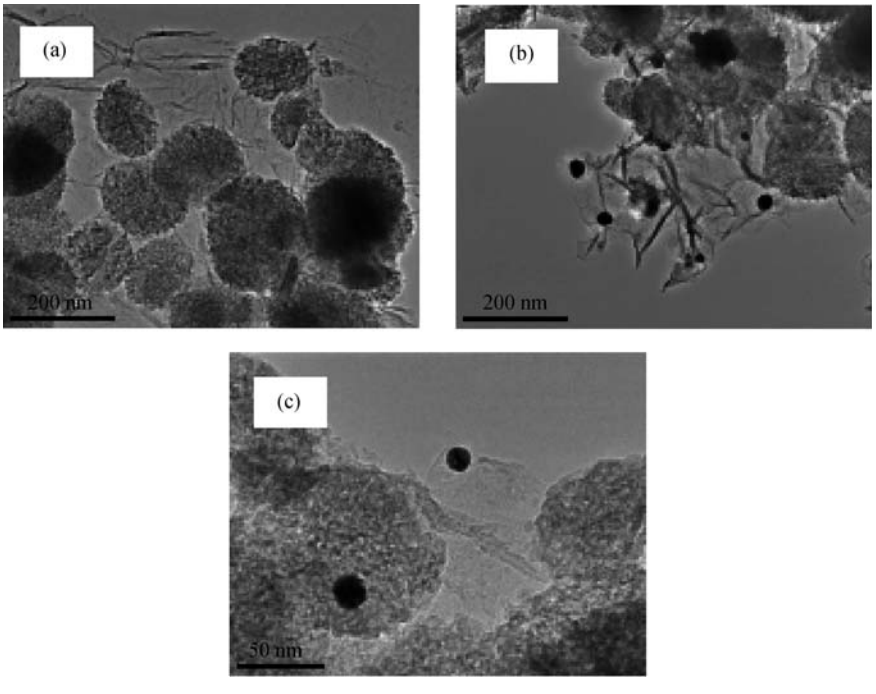

Fig. 2 TEM images of TiO_2/RGO before (a) and after (b) the deposition of Au nanoparticles. (c) A higher magnification TEM image of Au/TiO_2/RGO

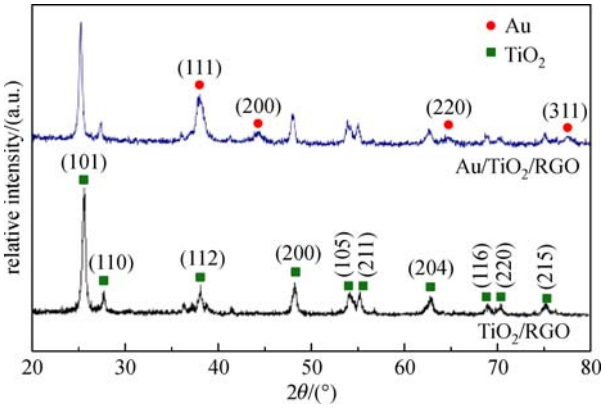

Fig. 3 XRD patterns of TiO_2/RGO and Au/TiO_2/RGO

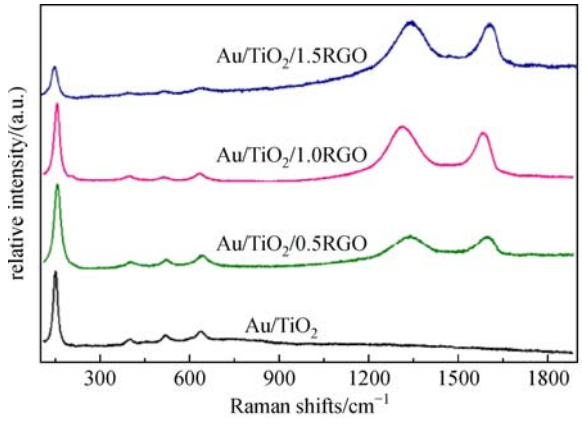

Fig. 4 Raman spectra of Au/TiO_2 and Au/TiO_2/RGO

capabilities of TiO_2 and Au/TiO_2 were also evaluated under the same conditions. It can be found from Fig. 5 that the degradation of phenol follows pseudo-first-order kinetics by the linear equation $\ln(C_0/C_t) = Kt$ (C_0 is the initial concentration of phenol, C_t is the concentration of phenol at time t, and K is the kinetic constant). Without any catalyst, the phenol degradation kinetic constant was 0.0021 h^{-1}. Using TiO_2 and Au/TiO_2 as photocatalysts, the kinetic constants reached 0.0043 and 0.0060 h^{-1}, respectively. This indicates that the photocatalyst plays a significant role in the phenol degradation, and an enhancement of the photocatalytic activity was achieved by the deposition of Au nanoparticles on TiO_2. Particularly, Fig. 5 shows that, compared with Au/TiO_2, the presence of RGO in Au/TiO_2/RGO had an obvious effect on the phenol degradation under the same experimental conditions. Even with a small amount of RGO, the kinetic constant increased to 0.0091 h^{-1} for Au/TiO_2/0.5RGO. When using Au/TiO_2/1.0RGO as a photocatalyst, the kinetic constant reached the highest value of 0.0107 h^{-1}, which was approximately 1.8 times that of Au/TiO_2. However, upon a further increase in the amount of RGO in Au/TiO_2/RGO, the kinetic constant decreased to 0.0081 h^{-1} for Au/TiO_2/1.5RGO, indicating a reduction of the photocatalytic activity. This observation could be ascribed to the introduction of a relatively high percentage of RGO in Au/TiO_2/RGO, which could result in a rapid decrease of light intensity reaching through the reaction solution. Therefore, a suitable content of RGO in Au/TiO_2/RGO nanocomposite is crucial for the photocatalytic performance, and the following experiments were conducted selecting Au/TiO_2/1.0RGO.

To determine the factors to deliver better a photocatalytic activity for Au/TiO_2/RGO, the charge transport resistance was characterized by EIS. Figure 6 shows the EIS plots of Au/TiO_2 and Au/TiO_2/RGO. In the dark, the arcs of both Au/TiO_2 and Au/TiO_2/RGO are very large. However, under UV light irradiation, the radii of the semicircles decreased because of the presence of charge carriers induced by the incident light [13]. Meanwhile, the semicircle of Au/TiO_2/RGO is smaller than that of Au/TiO_2. This result indicates that the charge transfer

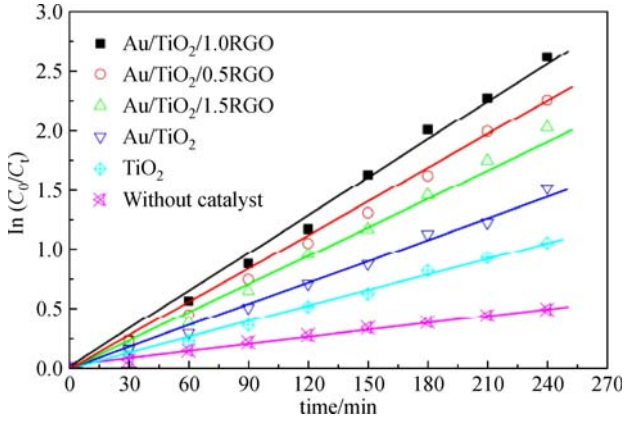

Fig. 5 Evaluation of phenol degradation under UV light (0.75 mW·cm^{-2}) irradiation for no catalyst, TiO_2, Au/TiO_2, Au/TiO_2/0.5RGO, Au/TiO_2/1.0RGO and Au/TiO_2/1.5RGO

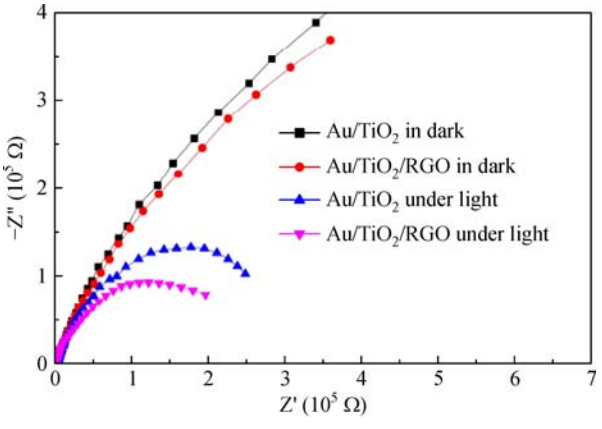

Fig. 6 Electrochemical impedance spectroscopy plots of Au/TiO_2 and Au/TiO_2/RGO both in the dark and under UV light (0.75 mW·cm^{-2}) irradiation

resistance in Au/TiO_2/RGO is relatively low in the presence of UV light irradiation, which would be beneficial for photocatalytic reactions.

Since the formation of H_2O_2 is a critical step for the photocatalytic reaction, the concentration of H_2O_2 in the reaction solution was detected. Figure 7 shows the concentration of H_2O_2 for no photocatalyst, TiO_2, Au/TiO_2, and Au/TiO_2/RGO. Without any photocatalyst, the concentration of H_2O_2 in water is approximately 0.00311 mmol·L^{-1} under UV light (0.75 mW·cm^{-2}) irradiation over 4 h. For TiO_2, the concentration of H_2O_2 is merely approximately 0.00868 mmol·L^{-1}. When using Au/TiO_2 as a photocatalyst, the concentration of H_2O_2 in water reaches approximately 0.122 mmol·L^{-1}. When using Au/TiO_2/RGO as a photocatalyst, the concentration of H_2O_2 in water reaches the highest value of approximately 0.335 mmol·L^{-1}, which was approximately 2.7 times that of Au/TiO_2, indicating that Au/TiO_2/RGO can produce more H_2O_2 than Au/TiO_2 during the photocatalytic process. This result demonstrated that, compared with Au/TiO_2, using RGO as a support could facilitate the transportation of the photogenerated electrons from TiO_2 across RGO to the Au nanoparticles at locations separated from the TiO_2 anchored sites, thus enhancing the separation of photogenerated electron-hole pairs.

To further investigate the difference of oxidative radicals in the photocatalytic reactions, an ESR technique was performed choosing DMPO as a spin-trap reagent. Figure 8 shows the ESR spectra of TiO_2, Au/TiO_2, and Au/TiO_2/RGO both in the dark and under UV light irradiation. In the dark, no ESR signals appeared. Under UV light irradiation, all samples showed quartet peaks with a 1:2:2:1 intensity pattern, which could be indexed to a DMPO-OH adduct [22]. This indicates that •OH is one of the main oxidative radicals in the photocatalytic reaction solution. Meanwhile, it can also be found from Fig. 8 that the peak intensity of Au/TiO_2/RGO is greater than that of Au/TiO_2 under the same experimental conditions, indicating that more •OH was produced for Au/TiO_2/RGO during the photocatalytic process. This result, in accordance with the H_2O_2 measurements (Fig. 7), demonstrates that a more efficient reduction of H_2O_2 to •OH occurred at the surface of the Au nanoparticles loaded on RGO and that a high photoactivity was achieved for Au/TiO_2/RGO.

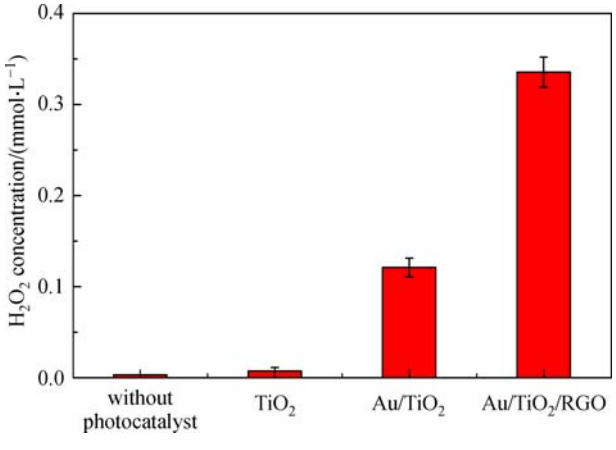

Fig. 7 The formation of H_2O_2 for no photocatalyst, TiO_2, Au/TiO_2, and Au/TiO_2/RGO under UV light (0.75 mW·cm^{-2}) irradiation for 4 h

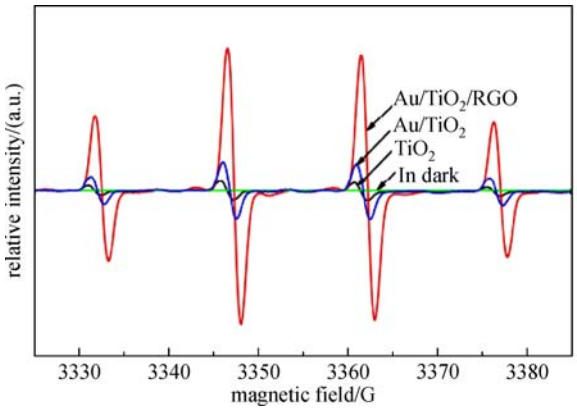

Fig. 8 ESR spectra of TiO_2, Au/TiO_2, and Au/TiO_2/RGO both in the dark and under UV light irradiation

The mechanism of RGO as a collector in graphene-based materials has been established [12,13,16–18,23]. Based on the results illustrated above, we believe that this mechanism could also explain reason for Au/TiO_2/RGO exhibiting a much higher photocatalytic activity than Au/TiO_2. Once RGO is introduced to Au/TiO_2/RGO, the selective loading of TiO_2 and Au at separate sites on RGO plays a key role for the enhancement of the photocatalytic activity because RGO has a beneficial structure for transporting photogenerated charge carriers, which effectively increases the separation of photogenerated electrons and holes. Meanwhile, RGO also provides more sites for the deposition of Au nanoparticles, resulting in photogenerated electrons producing more H_2O_2 as well as reducing H_2O_2 to form more •OH to participate in the photoredox reaction.

4 Conclusions

This work clearly demonstrated that an optimal amount of RGO in Au/TiO_2/RGO can dramatically enhance the photocatalytic performance of this material. The reason for this enhancement is that RGO is an attractive support for both TiO_2 and Au nanoparticles as well as a good electron transporter for affecting the photocatalytic capability. This work suggests that Au/TiO_2/RGO can be utilized in very appealing applications in several areas, such as solar cells, electronic nanodevices, water splitting, and environmental monitoring.

Acknowledgements This research was supported by the Natural Science

Foundation of Liaoning Province of China (No. 2014020149), the Scientific Research Project of Liaoning Provincial Department of Education (No. L201603) and the Open Foundation of Fujian Provincial Key Laboratory of Ecology-Toxicological Effects & Control for Emerging Contaminants (No. PY16005).

References

1. Hoffmann M R, Martin S T, Choi W, Bahnemannt D W. Environmental applications of semiconductor photocatalysis. Chemical Reviews, 1995, 95(1): 69–96
2. Nakata K, Fujishima A. TiO_2 photocatalysis: design and applications. Journal of Photochemistry and Photobiology C: Photochemistry Reviews, 2012, 13(3): 169–189
3. Wang H, Quan X, Yu H T, Chen S. Fabrication of a TiO_2/carbon nanowall heterojunction and its photocatalytic ability. Carbon, 2008, 46(8): 1126–1132
4. Hashimoto K, Irie H, Fujishima A. TiO_2 photocatalysis: a historical overview and future prospects. Japanese Journal of Applied Physics, 2005, 44(12): 8269–8285
5. Mor G K, Shankar K, Paulose M, Varghese O K, Grimes C A. Use of highly-ordered TiO_2 nanotube arrays in dye-sensitized solar cells. Nano Letters, 2006, 6(2): 215–218
6. Ge M, Guo C, Zhu X, Ma L, Han Z, Hu W, Wang Y. Photocatalytic degradation of methyl orange using ZnO/TiO_2 composites. Frontiers of Environmental Science & Engineering, 2009, 3(3): 271–280
7. Wang S, Wang K, Jehng J, Liu L. Preparation of TiO_2/MCM-41 by plasma enhanced chemical vapor deposition method and its photocatalytic activity. Frontiers of Environmental Science & Engineering, 2012, 6(3): 304–312
8. Tian Y, Tatsuma T. Mechanisms and applications of plasmon-induced charge separation at TiO_2 films loaded with gold nanoparticles. Journal of the American Chemical Society, 2005, 127(20): 7632–7637
9. Méndez-Medrano M G, Kowalska E, Lehoux A, Herissan A, Ohtani B, Rau S, Colbeau-Justin C, Rodríguez-López J L, Remita H. Surface modification of TiO_2 with Au nanoclusters for efficient water treatment and hydrogen generation under visible light. Journal of Physical Chemistry C, 2016, 120(43): 25010–25022
10. Gołąbiewska A, Malankowska A, Jarek M, Lisowski W, Nowaczyk G, Jurga S, Zaleska-Medynska A. The effect of gold shape and size on the properties and visible light-induced photoactivity of Au-TiO_2. Applied Catalysis B: Environmental, 2016, 196: 27–40
11. Stankovich S, Dikin D A, Dommett G H B, Kohlhaas K M, Zimney E J, Stach E A, Piner R D, Nguyen S T, Ruoff R S. Graphene-based composite materials. Nature, 2006, 442(7100): 282–286
12. Perreault F, Fonseca de Faria A, Elimelech M. Environmental applications of graphene-based nanomaterials. Chemical Society Reviews, 2015, 44(16): 5861–5896
13. Zhang N, Yang M Q, Liu S, Sun Y, Xu Y J. Waltzing with the versatile platform of graphene to synthesize composite photocatalysts. Chemical Reviews, 2015, 115(18): 10307–10377
14. Zhang H, Lv X, Li Y, Wang Y, Li J. P25-graphene composite as a high performance photocatalyst. ACS Nano, 2010, 4(1): 380–386
15. Zhang N, Zhang Y, Xu Y J. Recent progress on graphene-based photocatalysts: current status and future perspectives. Nanoscale, 2012, 4(19): 5792–5813
16. Tu W, Zhou Y, Zou Z. Versatile graphene-promoting photocatalytic performance of semiconductors: Basic principles, synthesis, solar energy conversion, and environmental applications. Advanced Functional Materials, 2013, 23(40): 4996–5008
17. Xiang Q, Yu J, Jaroniec M. Synergetic effect of MoS_2 and graphene as cocatalysts for enhanced photocatalytic H_2 production activity of TiO_2 nanoparticles. Journal of the American Chemical Society, 2012, 134(15): 6575–6578
18. Liu Y, Yu H, Wang H, Chen S, Quan X, Efficient H. 2 production over Au/graphene/TiO_2 induced by surface plasmon resonance of Au and band-gap excitation of TiO_2. Materials Research Bulletin, 2014, 59: 111–116
19. Yuan J, Shiller A M. Determination of subnanomolar levels of hydrogen peroxide in seawater by reagent-injection chemiluminescence detection. Analytical Chemistry, 1999, 71(10): 1975–1980
20. Wang H, Zhang X, Su Y, Yu H, Chen S, Quan X, Yang F. Photoelectrocatalytic oxidation of aqueous ammonia using TiO_2 nanotube arrays. Applied Surface Science, 2014, 311: 851–857
21. Kotal M, Bhowmick A K. Multifunctional hybrid materials based on carbon nanotube chemically bonded to reduced graphene oxide. Journal of Physical Chemistry C, 2013, 117(48): 25865–25875
22. Wang H, Su Y, Zhao H, Yu H, Chen S, Zhang Y, Quan X. Photocatalytic oxidation of aqueous ammonia using atomic single layer graphitic-C_3N_4. Environmental Science & Technology, 2014, 48(20): 11984–11990
23. Yu H, Ma B, Chen S, Zhao Q, Quan X, Afzal S. Electrocatalytic debromination of BDE-47 at palladized graphene electrode. Frontiers of Environmental Science & Engineering, 2014, 8(2): 180–187